Journal of Fluorescence, Vol. 9, No. 2, 1999

The LIF Excitation Spectrum of Jet-Cooled 2,6-Dicyano-3, 5-Dimethylaniline

P. Kolek,[1] P. Gajdek,[1] T. Motylewski,[1] M. Tulej,[1] and J. Najbar[1]

Received August 7, 1998; accepted November 23, 1998

The laser-induced fluorescence (LIF) excitation spectrum of jet-cooled 2, 6-dicyano-3,5-dimethylaniline (DCDMA) has been measured in the spectral range of 29,750–32,250cm^{-1}. The band origin at 29,860.8 cm^{-1} and as many as 250 vibrational bands have been identified in the excitation spectrum. The analysis of the excitation spectrum of DCDMA gives more than 28 vibrational modes involving aromatic ring oscillations and oscillations related to the substituent groups. DCDMA is nonplanar in the ground state, with the NH_2 plane at about 9° with respect to the molecular plane (RHF/6-31G*). The singlet excited molecule is planar (CIS/6-31G*). Both CIS/6-31G* and CASPT2 calculations predict that the lowest excited state of DCDMA involves a dominant HOMO-LUMO excited configuration. The characteristic feature of the excitation spectrum of DCDMA is the presence of progressions in the low-frequency mode, 112 cm^{-1}. The calculations suggest that this mode and some other active modes involve motions of the amino group and strongly interacting adjacent cyano substituents.

KEY WORDS: LIF excitation spectrum; supersonic jet; ab initio geometries; Dushinsky effect; intramolecular hydrogen bonding.

INTRODUCTION

The applications of laser techniques to the UV/VIS range and supersonic jet expansion to the spectroscopy of organic molecules have contributed greatly to the evaluation of potential energy surfaces in their ground electronic state and, especially, potential surfaces for excited electronic states as well as vibronic couplings between different electronic states [1–6]. Although spectroscopic information is limited to the Franck–Condon zone, the equilibrium geometries of the excited states can, in favorable circumstances, be readily evaluated from the spectral data [7–13]. The benzene aromatic ring represents a rigid structure, undergoing small geometry expansion upon electronic excitation. Excited states and intramolecular dynamics in substituted benzene have been the subjects of many studies [13–25]. Among substituted benzene molecules, the aniline molecule and its derivatives are of fundamental interest for many reasons. They undergo large geometry changes between the ground and the excited electronic states [8,17,19,21,24,26–28]. Aniline is nonplanar in the ground electronic state, with the NH_2 plane at 42° with respect to the ring plane. The ground-state potential energy surface shows a double minimum in the inversion mode. In the lowest singlet excited state the aniline molecule is planar. The corresponding potential function in the inversion mode is anharmonic, having a very small barrier at planar geometry. There is a nearly twofold increase in this mode frequency between the ground and the excited state for the isolated aniline molecule. Due to these geometry and frequency changes, the fluorescence excitation spectrum of the jet-cooled aniline molecule shows significant intensity of the bands correlating with the inversion mode [8,17].

Recently, ab initio electronic structure calculations have been performed by Sobolewski *et al.* [29] to characterize the charge transfer process in benzonitrile, 4-amino-

[1] Department of Physical Chemistry and Electrochemistry, Jagiellonian University, 3 Ingardena, 30-060 Cracow, Poland.

1053-0509/99/0600-0123$16.00/0

bezonitrile, and 4-dimethylaminobezonitrile. Geometry optimizations of the singlet excited charge-transfer states predict a planar configuration with a bent CN group. The rehybridization of the carbon atom of the cyano group is largely responsible for the stabilization of the lowest CT state. The contribution of higher excited states to the spectral behavior of the lowest excited state and generally the vibronic coupling between excited electronic states are very important issues for elucidation of the photo-transformations of benzene and its derivatives [20].

2,6-Dicyano-3,5-dimethylaniline (DCDMA), having two cyano groups next to the amino group, shows very different properties from those characteristic for aniline. The interactions between the amino group and the cyano groups in the DCDMA molecule induce significant rehybridization at the nitrogen atom and its basicity compared to the aniline molecule. The equilibrium constant for the protonation of DCDMA is very small, with a pK_a at of about -10.

The purpose of this work is to investigate the ground state and the lowest singlet excited state of DCDMA using spectroscopy and ab initio quantum mechanical calculations. We report the fluorescence excitation spectra of jet-cooled DCDMA in the spectral range of 29,750–32,250 cm^{-1}. Quantum mechanical ab initio calculations and analysis of the progressions observed in the spectrum have allowed for assignment of the majority of the vibrational modes. The modes present in the fluorescence excitation spectrum include vibrations of the aromatic ring as well as many modes due to interacting substituents of the benzene ring.

EXPERIMENTAL

For excitation of the fluorescence emission a HY 400 Nd:YAG laser and a dye laser DY 300 (Lumonics) were used. The pulses from the dye laser at 10 Hz were 10 ns in duration and 20 mJ of energy per pulse, with a band width of about 0.1 cm^{-1}. The frequency-doubled (BBO) output of the dye laser operating with DCM in methanol:propylene carbonate (1:1) was used to excite DCDMA fluorescence. The laser beam is introduced to a vacuum chamber by an $f = 300$-mm silica fused lens and crossed the seeded supersonic expansion 10 mm downstream from a needle 25 mm long having a 0.25-mm internal diameter. A General Valve device was used for pulsed operation of the free expansion. The data acquisition and control of our experimental setup were performed using a CAMAC electronic system controlled by an AT 486 microcomputer. A CAMAC 712 pulse analyzer was used to measure pulses delivered from a cooled Thorn EMI 9558QB photomultiplier. Three different triggering pulses at 10 Hz were generated and independently delayed by a specially designed CAMAC module. The first pulse was used to trigger a Nd:YAG laser and dye laser; the second was used to trigger the operation of the supersonic jet valve. The third pulse was used to trigger a CAMAC 712 analog-to-digital converter. A digital power meter was use to monitor the energies of the dye laser pulses. The computer programs in Pascal were developed for data acquisition, additional signal averaging, and spectral corrections. Argon or helium was used as carrier gas. The sample injection system was heated at 140°C.

Samples of DCDMA were synthesized using the procedure described in Ref. 30. The structure of this compound was verified using IR, Raman, and NMR methods. Deuterium exchange in DCDMA was achieved by multiple recrystalization of this compound from boiling deuterated ethanol (C_2H_5OD) with a small amount of D_2O. The deuteration exchange in the amino group was confirmed by IR spectroscopy. For the deuterated sample of DCDMA the injection system was heated at 180°C.

The quantum mechanical calculations were performed at the Jagiellonian University Computer Center Cyfronet using a CONVEX computer and at Bergen University, Norway.

RESULTS AND DISCUSSION

DCDMA Geometry and Vibrational Frequencies

The ground and the lowest singlet excited-state geometry of DCDMA and the normal mode frequencies in these two electronic states have been evaluated by ab initio calculation using GAUSSIAN 94 program. The S_0 and S_1 molecular geometries of DCDMA are shown in Fig. 1. The largest geometry changes upon electronic excitation are connected with the amino group. In Fig. 1 the bond length for the ground states of DCDMA are given on the left side of the formula. On the right side of the formula the changes in the bond lengths for the transition S_0–S_1 are shown. The DCDMA molecule is nonplanar in the ground electronic state, with the NH_2 plane at 9^0 with respect to the ring plane (RHF/6-31G*), C_s. In the excited state the DCDMA molecule is planar (RCIS/6-31G*), C_{2v}. The lowest singlet excited state of DCDMA is of p character, with a dominant contribution from a HOMO-LUMO configuration. This conclusion agrees well with the photophysical behavior of DCDMA in cyclohexane solution. The fluorescence quantum yield, 0.25, and the fluorescence lifetime, 3.07 ns, give 12.3 ns for the radiative fluorescence lifetime of the lowest

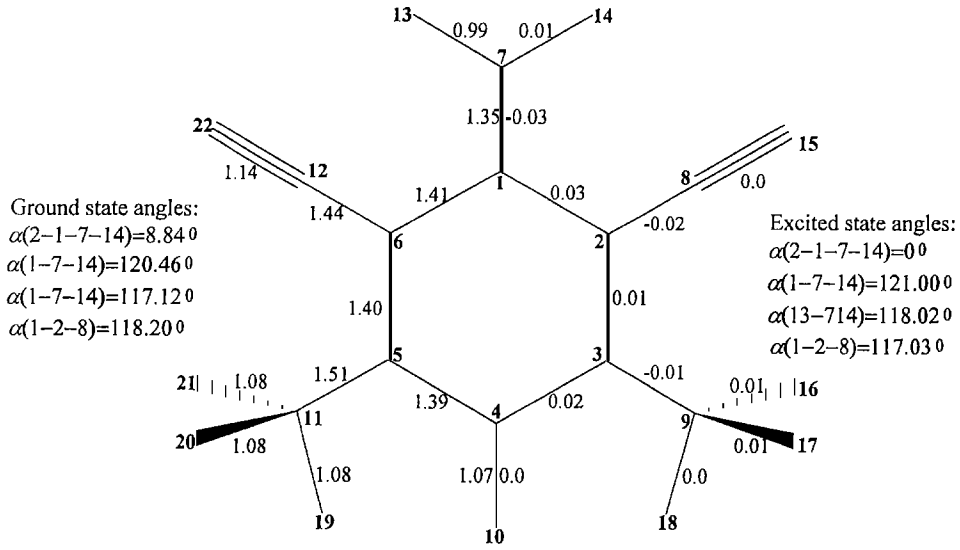

Fig. 1. The DCDMA ground-state geometry (HF/6-31G*; left side) and the geometry change for the S_0–S_1 exitation (CIS/6-31G*; right side).

excited state of DCDMA. The radiative fluorescence lifetime evaluated from the integral absorption intensity was found to be equal ca. 10 ns.

The RCIS/6-31G* calculation predicts the S_1 energy at 4.99 eV. Much better evaluation of the lowest singlet excited-state energy has been obtained using the CASSCF [31] and CASPT2 [32,33] methods from the MOLCAS3 program with a contracted ANO basis set: C, N (10s6p3d)/[3s2p1d], H 7s/2s. The calculated energies of the S_1 state are at 4.37 eV (CASSCF) and 3.68 eV (CASPT2). The latter value is very close to the experimental value 3.702 eV corresponding to the 00 transition in the DCDMA excitation spectrum. In both calculations 12 orbitals antisymmetric to the molecular plane were active. In the first preliminary computation 8 occupied orbital were active: 3 π of the aromatic ring, 2π(C≡N), 1 nitrogen lone pair, 2 σ (CH_3), and 4 virtual. In the final calculation, three orbitals with the highest occupation numbers and the lowest energies, 2 σ(CH_3) and the nitrogen lone pair, were inactive, and seven virtual orbitals were active.

The equilibrium geometry and Hessian matrix derived from ab initio calculations give good characteristics of the potential energy function of the molecule in the corresponding electronic state [9,10, 12,13,28,34–37]. The limitations concern some vibrational modes involving, e.g., the inversion mode or some other large-amplitude motions. Upon electronic excitation both the equilibrium geometry and the force field are changed. Within harmonic approximation the situation can be conveniently described using the displacement vector and the rotation matrix, giving the transformation of the normal vibrational coordinates after electronic excitation. The normal coordinates in the ground state (g) and in the excited state (e) are given by displacements in Cartesian coordinates from the equilibrium geometry in the corresponding electronic state, g or e. They are expressed by the following relations [38]:

$$Q_j^{g(e)} = \sum_{k=1}^{3N} l_{jk}^{g(e)}(q_k - q_k^{g(e)})$$

where Q_i are normal coordinates and q_k are Cartesian coordinates of the atoms.

The normal coordinates in the two electronic states are related as follows:

$$Q_i^e = D_i + \sum_{j=1}^{3N} R_{ij} Q_j^g$$

where the displacement vector of the normal coordinates is given by

$$D_i = \sum_{k=1}^{3N} l_{ik}^e (q_k^e - q_k^g)$$

whereas the rotation matrix is expressed as follows:

$$R_{ij} = \sum_{k=1}^{3N} l_{ik}^e (l^{gT})_{kj}$$

The rotation matrix gives a very convenient measure of the normal mode correlations and their mixing upon electronic excitation (Dushinsky effect).

The normal mode frequencies have been calculated for the S_0 and S_1 electronic states using the RHF/6-31G*

and RCIS/6-31G* methods, respectively. The present calculations predict that electronic excitation induces small frequency changes (1% decrease) except for the modes involving motions of the amino group and some skeletal modes [5,28,36]. The calculated ground-state mode frequencies for the DCDMA molecule have been compared with the frequencies determined from IR and Raman spectra measured for crystalline DCDMA, but the calculated frequencies were found to be too high. The scaling factor was found to be 0.856. The corresponding scaling factor ($0.99 \times 0.856 = 0.845$) has been applied to the S_1 mode frequencies. The calculated normal mode frequencies for the ground and excited electronic states are given in Table I. The ground-state frequencies are numbered according to their increasing values. This numbering of the vibrational modes is used in subsequent discussion. The S_1 vibrational frequencies have been assigned to the corresponding S_0 modes by comparing the overlap of the normal mode motions in these two electronic states.

The components of the displacement vector are given in Fig 2a. They are arranged according to increasing normal mode frequencies in the ground electronic state. In Fig. 2b the elements of the Dushinsky rotation matrix are shown. In Fig. 2b the normal modes are grouped according to four irreducible representations of the C_{2v}

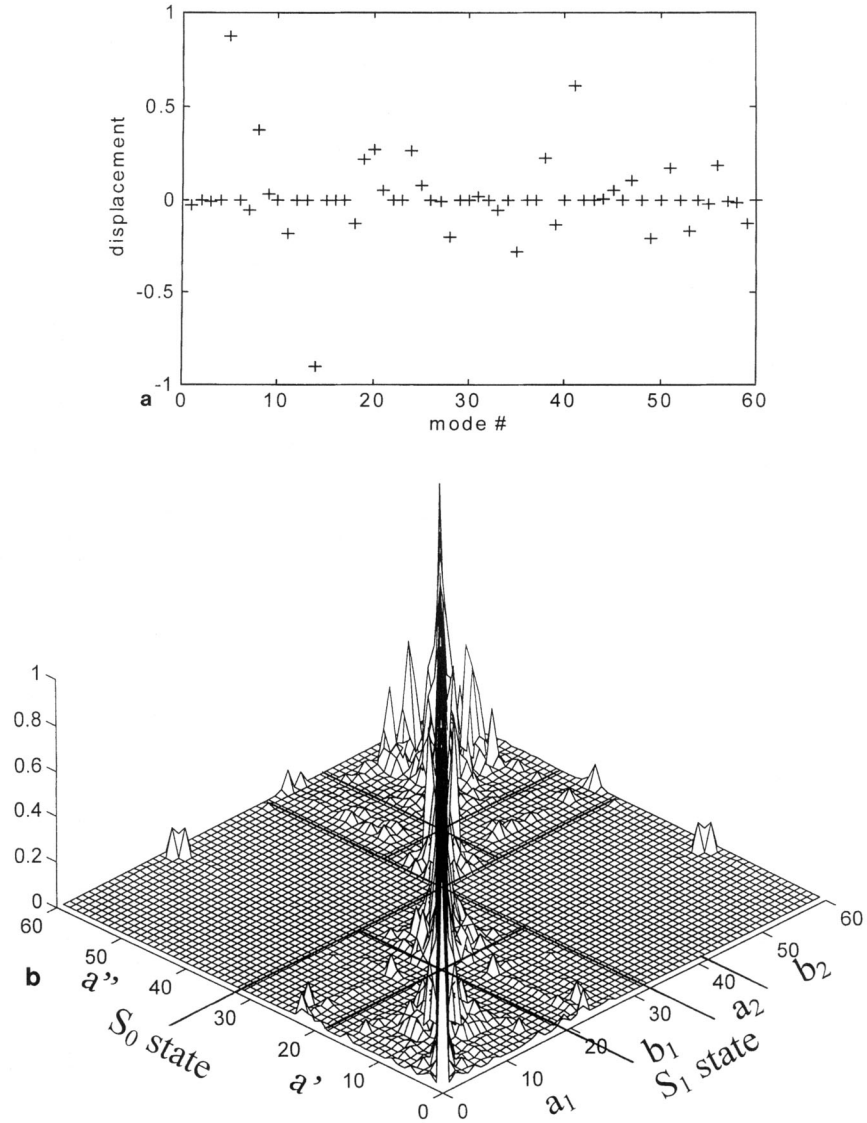

Fig. 2. Characteristics of the geometry change for the S_0–S_1 transition of DCDMA in terms of the normal modes: (a) the mode displacement vector; (b) the rotation matrix.

Table I. The Vibrational Frequencies for DCDMA in the Ground Electronic State S_0 (HF/6-31G*) and in the Excited Electronic State S_1 (CIS/6-31G*)

	S_0 state			S_1 state		
Mode No.	C_s symmetry	ν (cm^{-1})	$\nu \cdot 0.855$ (cm^{-1})[a]	C_{2v} symmetry	ν (cm^{-1})	$\nu \cdot 0.846$ (cm^{-1})[a]
1	a′	90	77	b_1	87	74
2	a″	94	81	a_2	55	47
3	a′	104	89	b_1	124	105
4	a″	107	92	a_2	129	110
5	a′	137	117	a_1	137	116
6	a″	173	148	b_2	171	144
7	a′	196	167	b_1	162	137
8	a′	206	176	b_1	608	515
9	a′	271	232	b_1	230	195
10	a″	285	243	a_2	232	196
11	a′	303	259	a_1	286	242
12	a″	332	283	b_2	322	272
13	a″	442	378	b_2	400	338
14	a′	461	394	a_1	456	386
15	a″	468	400	a_2	687	581
16	a″	507	433	b_2	509	431
17	a″	557	476	a_2	415	351
18	a′	570	488	b_1	551	466
19	a′	580	496	a_1	579	490
20	a′	628	537	a_1	616	521
21	a′	672	574	b_1	451	381
22	a″	706	604	b_2	700	592
23	a″	711	607	a_2	556	471
24	a′	715	612	a_1	707	598
25	a′	856	732	b_1	731	619
26	a″	873	746	b_2	852	721
27	a′	936	800	b_1	928	785
28	a′	1078	921	a_1	1058	895
29	a″	1111	950	b_2	1150	973
30	a″	1154	986	b_2	1033	874
31	a′	1167	998	b_1	1150	973
32	a″	1170	1000	a_2	1133	959
33	a′	1189	1017	a_1	1191	1008
34	a″	1234	1055	b_2	1195	1011
35	a′	1321	1130	a_1	1333	1128
36	a″	1323	1131	b_2	1763	1491
37	a″	1374	1175	b_2	1346	1139
38	a′	1473	1259	a_1	1450	1227
39	a′	1563	1337	a_1	1561	1321
40	a″	1567	1340	b_2	1566	1325
41	a′	1576	1348	a_1	1586	1342
42	a″	1624	1388	b_2	1615	1367
43	a″	1628	1392	a_2	1616	1367
44	a′	1629	1393	b_1	1617	1368
45	a′	1634	1397	a_1	1635	1383
46	a″	1653	1414	b_2	1637	1385
47	a′	1749	1495	a_1	1692	1431
48	a″	1779	1521	b_2	1409	1193
49	a′	1840	1573	a_1	1854	1568
50	a″	2583	2208	b_2	2469	2088
51	a′	2583	2208	a_1	2510	2124
52	a″	3219	2752	b_2	3181	2691
53	a′	3219	2752	a_1	3183	2693
54	a″	3279	2803	a_2	3223	2727
55	a′	3279	2804	b_1	3224	2727
56	a′	3306	2827	a_1	3284	2778
57	a″	3307	2827	b_2	3284	2778
58	a′	3386	2895	b_1	3381	2860
59	a′	3834	3278	a_1	3787	3204
60	a″	3953	3380	b_2	3909	3307

[a] Scaled frequency.

point group appropriate for the geometry of the DCDMA molecule in the singlet excited state. The ordering of the normal modes in the excited state in each irreducible representation was permutated to bring the largest elements of the Dushinsky matrix to the diagonal position. The resulting correlation of the normal modes in these two electronic states is given in Table I. Figure 2b also shows that this electronic excitation involves some mode mixings. They are represented by the off-diagonal elements of the Dushinsky rotation matrix.

Some mode frequencies, predominantly those connected with the amino group, undergo significant change upon excitation. One should note that the present calculation correctly predicts the frequency change upon excitation for the vibrational mode, which involves ring, deformations toward two Kekule structures of the benzene ring [39]. This mode, 1131 cm^{-1} (S_0) and 1491 cm^{-1} (S_1), involves motion of the skeleton carbon atoms. Assigned values are 1183 and 1494 cm^{-1}, which compare very well with the above calculated and scaled frequencies.

The LIF Excitation Spectrum of the DCDMA Molecule

The UV absorption and fluorescence spectra of the DCDMA in solution show small Stokes shifts. The absorption spectrum of the DCDMA in cyclohexane at 293 K shows a ca. 600-cm^{-1} bathochromic shift compared with the vapor phase absorption at 433 K. The fluorescence excitation spectrum of jet-cooled DCDMA in the 29,750- to 32,250-cm^{-1} spectral range is shown in Fig 3. For the argon carrier gas the bandwidths of the vibronic lines are about 2 cm^{-1}. For helium as the carrier gas at 4 atm of stagnation pressure, line widths of about 1.4 cm^{-1} were obtained. The strongest transition, at 29,860.8 cm^{-1} (bandwidth, 1.5 cm^{-1}), corresponds to the

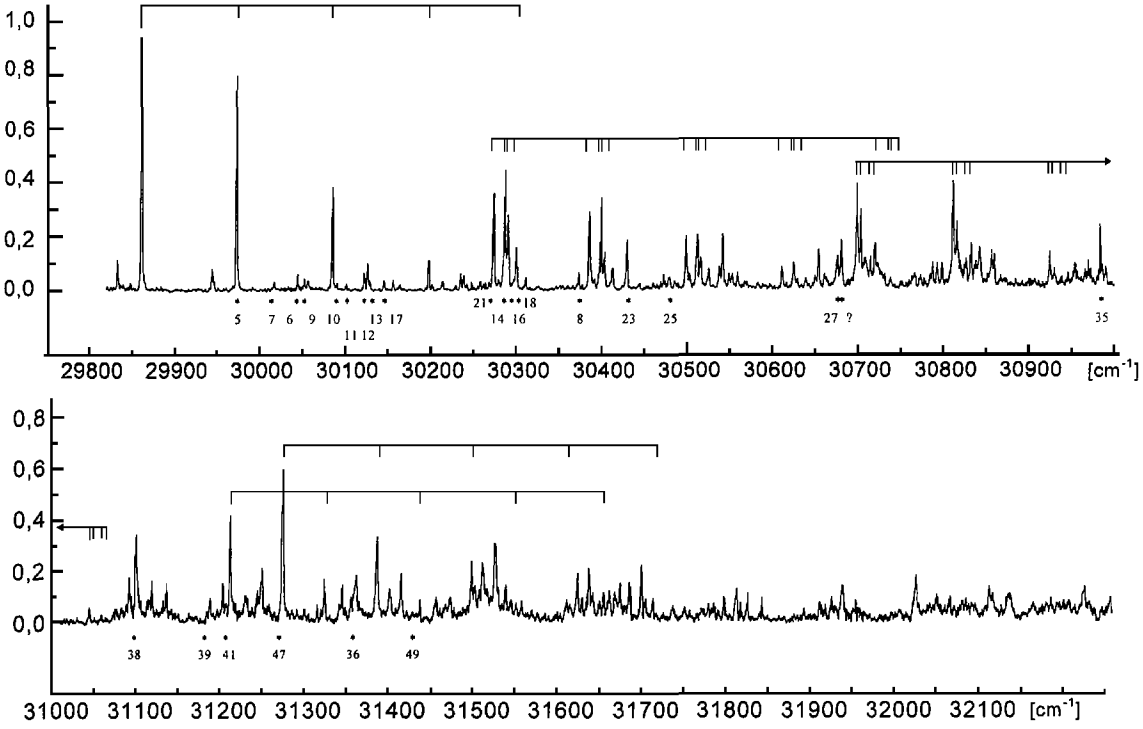

Fig. 3. The LIF excitation spectrum of DCDMA cooled by argon expansion.

band origin. Two low-intensity satellite transitions have been found, at -28 and -12 cm^{-1}, below the strong 00 transition. Their intensities depend on the carrier gas used in the supersonic expansion. In Fig. 4 the excitation spectra of DCDMA in the 00 region are shown for argon and helium carrier gases. For helium a significant reduction of the -28-cm^{-1} band intensity is observed. Similar results have been obtained for the supersonic expansion using nitrogen as a carrier gas. The increase in stagnation pressure reduces the intensity of the satellite bands. These results suggest that the bands at -28 cm^{-1} and -12 cm^{-1} from the 00 transition are hot bands due to incomplete cooling of the vibrational modes in the ground state of the DCDMA molecule.

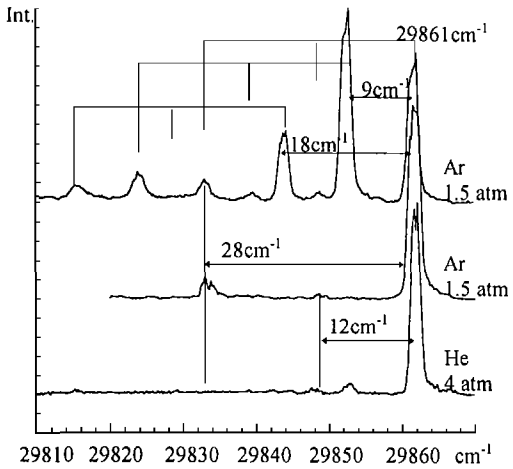

Fig. 4. The 00 transition region of the excitation spectrum of jet-cooled DCDMA-h_2 using Ar or He as the carrier gas and DCDMA-d_2 using Ar as the carrier gas.

In Fig. 4 the fluorescence excitation spectrum obtained for partially deuterated sample of DCDMA using argon carrier gas is also shown. The strong lines occurring at 29,852.5 and at 29,843.8 cm^{-1} can be tentatively assigned to DCDMA molecules containing –NDH and –ND_2 amino groups, respectively. The corresponding deuteration shifts of the 00 transition are equal to -9 cm^{-1} for the DCDMA molecule containing a singly deuterated amino group and -18 cm^{-1} for doubly deuterated species. The deuteration shifts observed here are larger than that found for 1-aminonaphthatene $+1.5$ and -3.5 cm^{-1} for singly and doubly deuterated species, respectively [40]. The deuteration shifts observed for the DCDMA molecule are comparable to those observed for the exchange of the hydrogen atoms bonded to the aromatic ring or for the deuterium exchange in methyl groups (e.g., in toluene). Large shifts of the 00 transition due to deuteration of the amino group in DCDMA suggest strong interaction of hydrogen atoms of the amino group with

two cyano groups. In the excitation spectrum for the partially deuterated sample of DCDMA shown in Fig. 4, the hot bands for each chemical species can be recognized.

About 250 vibrational bands can be identified in the spectrum in Fig. 3. The characteristic feature of this excitation spectrum is the presence of progressions with the spacing 112 cm^{-1}. The progression in the 112-cm^{-1} mode appears in combination with many other vibrational frequencies. The proposed band assignments are based on more than 25 fundamental frequencies. These fundamental frequencies are indicated in Fig. 3. They are collected in Table II. The proposed assignments of the excited-state fundamental vibrations are also presented in Table II [41]. Some evaluation of the present assignment can be gained from Fig. 5, where the fundamental frequencies identified in the the DCDMA excitation spectrum are compared with the corresponding calculated mode frequencies. The assignments find support for the nonzero values of the components of the displacement vector for the S_0–S_1 electronic transition. The characteristic mode 112 cm^{-1} can be easily identified with the mode involving in-plane symmetrical motion of two cyano groups adjacent to the amino group. Moreover, three other strong transitions, at 426, 1344, and 1569 cm^{-1} from the 00 transition, have significant intensities. Using the displacement vector these vibronic transitions have been assigned vibrations 14, 41, and 49 (a′ symmetry). The other fundamentals were assigned to the calculated modes using the frequency correlations. The resulting assignment of the vibrational modes for the DODCA molecule in the singlet excited state is given in Table II. In Fig. 6 the mode patterns for 10 fundamental vibrational modes appearing in the LIF excitation spectrum of DCDMA with intensities greater than 20% of the intensity of the 00 transition are shown.

Comparing the correlation presented in Fig. 5, it seems that there exists a very good correlation between the frequencies derived from the excitation spectrum and the vibrational mode frequencies obtained from the ab initio quantum mechanical calculation (after appropriate scaling) for vibrational frequencies above 500 cm^{-1}.

Table II. Assignment of the S_1 Fundamental Modes of DCDMA

Mode No. and symmetry	S_1 frequency	Displacement parameter	Calc. S_1 frequency	Calc. displacement parameter	Correlation with benzene modes
5 a′ (a1)	112	0.78	116	0.765	
7 a′ (b1)	156	0.03	137	0.003	
6 a″ (b2)	184		144		
9 a′ (b1)	191	0.04	195	0.001	17b
10 a″ (a2)	229		196		10a
11 a′ (a1)	240	0.02	242	0.03	18a
12 a″ (b2)	262		272		9b
13 a″ (b2)	266		338		6b
17 a″ (a2)	285		351		17a
21 a′ (b1)	412	0.37	381	0.003	5
14 a′ (a1)	426	0.60	386	0.817	6a
16 a″ (b2)	429		431		3
18 a′ (b1)	439	0.16	466	0.016	10b
19 a′ (a1)	494	0.02	490	0.047	
8 a′ (b1)	513	0.07	515	0.139	
20 a′ (a1) and 5 + 21	525	0.29	521	0.074	12
23 a″ (a2)	569		581		
24 a′ (a1) and 5^3 + 12	599	0.02	598	0.071	
25 a′ (b1)	618	0.04	619	0.006	
27 a′ (b1)	815	0.13	785	0.000	11
	820	0.18			
35 a′ (a1)	1122	0.25	1127	0.075	2
38 a′ (a1)	1233	0.37	1227	0.051	19b
39 a′ (a1)	1321	0.11	1321	0.018	7a
41 a′ (a1)	1344	0.44	1342	0.377	
47 a′ (a1)	1407	0.63	1431	0.011	15
36 a″ (b2)	1494		1491		14
49 a′ (a1)	1569	0.10	1568	0.040	

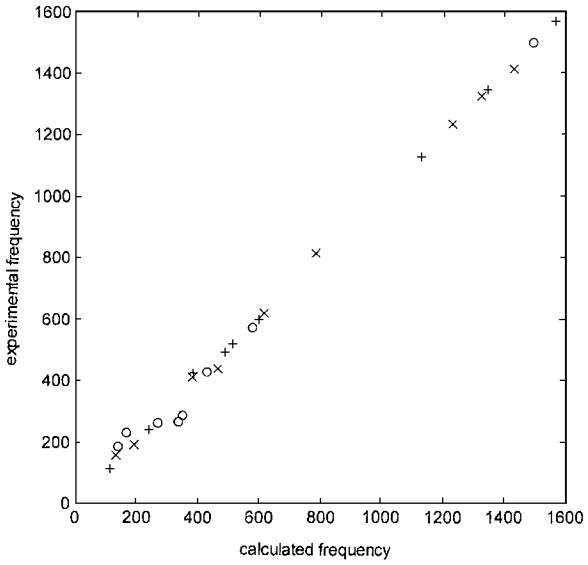

Fig. 5. The correlation between S_1 fundamental frequencies derived from the LIF excitation spectrum and the scaled ab initio CIS/6-31G* results: (+) normal modes where the intensity of the corresponding transition is well reproduced; (×) modes where the intensity is not satisfactorily reproduced in the calculations; (○) non-totally symmetric modes.

However, for some modes in the range 200–500 cm^{-1} significant discrepancies between frequencies derived from the excitation spectrum and the calculated values are observed. There is a deficiency of the calculated vibrational modes (using the scaling factor 0.845) in this frequency range.

Some vibrational modes in Table II belong to a″ symmetry. Their presence indicates vibronic coupling between the singlet excited state and other excited states of A′ symmetry. For DCDMA a′ symmetry vibrational modes may be involved in the vibronic coupling between excited states of the same symmetry. The latter coupling may substantially alter the intensities of the allowed vibronic transitions. A number of the vibrational modes assigned to a′ symmetry have much lower intensities than those predicted from ab initio CIS/6-31G* calculations (see columns 3 and 5 in Table II). These are the fundamental modes 412, 439, 1233, and 1407 cm^{-1}. To a large extent the observed regular structure of the fluorescence excitation spectrum of the DCDMA molecule can be accounted for using a single potential energy surface for the singlet excited state and invoking the Herzberg–Teller coupling mechanism [7].

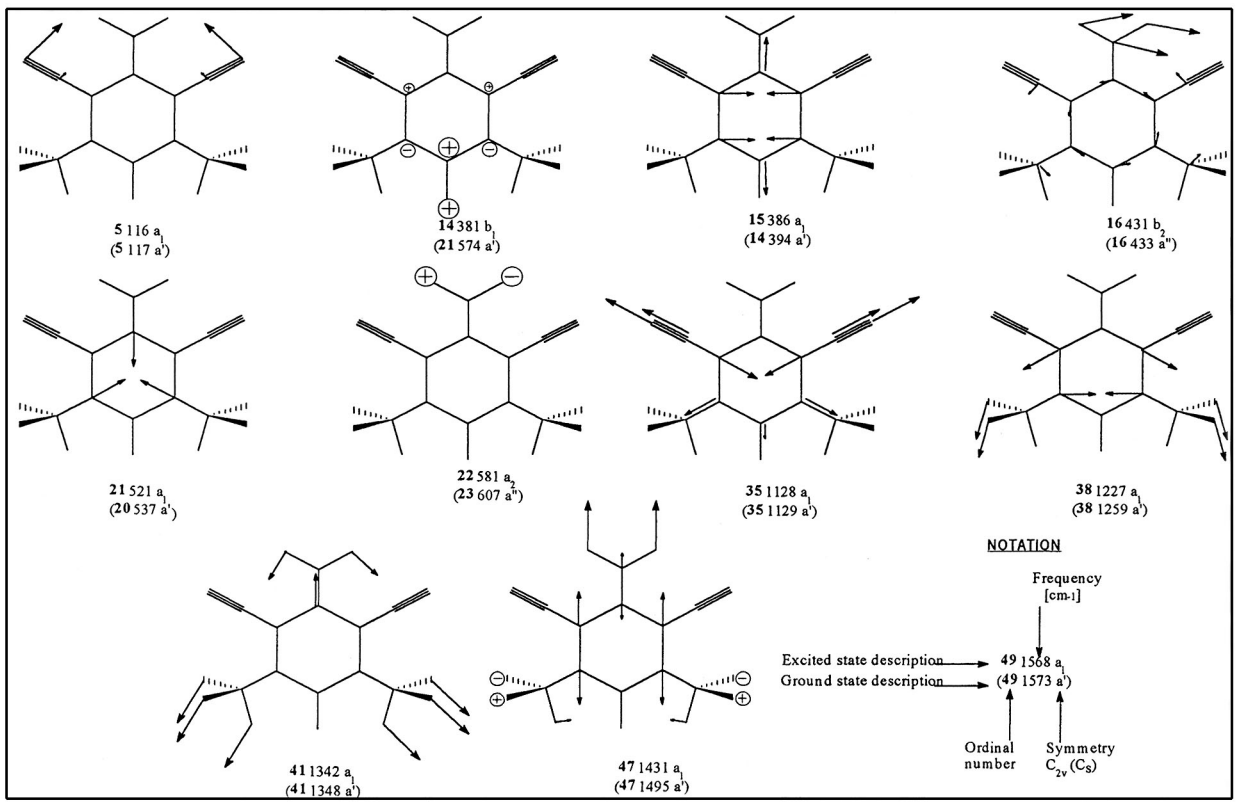

Fig. 6. The normal mode patterns for the fundamentals appearing in the LIF excitation spectrum with intensities greater than 0.2 of the 00 transition intensity.

The fluorescence excitation spectrum of DCDMA shows the presence of many vibrational modes involving the substituents of the phenyl ring. These modes involve bending of the nitrile group (motion inducing rehybridization at the carbon atom of the cyano group), as well as the symmetric motion of two cyano group and adjacent substituents (amino group and two methyl groups). A particularly strong interaction occurs between the amino group and two adjacent cyano groups. In the ground state of DCDMA this interaction is responsible for the extremely weak basicity of the amino group. Upon electronic excitation the changes in the interactions cause a significant change in the geometry of the excited DCDMA molecule. In the excited state the amino group is planar, with a substantially shortened C–N bond length. These geometry changes give rise to the long progression in 112 cm^{-1}.

The characteristic feature of the aromatic amines is the presence of the inversion mode in the amino substituent. Both semiempirical AM1 and ab initio quantum mechanical calculations using harmonic approximations are inadequate to predict the mode frequency in the ground state and in the excited state of the aniline molecule. Ab initio RCIS/6-31G* calculation gives two high-frequency 720 cm^{-1} (after scaling) compared with the 351 cm^{-1} observed in the fluorescence excitation spectrum of jet-cooled aniline.

The vibrational frequency 521 cm^{-1} derived from the excitation spectrum of DCDMA seems to agree with the 513 cm^{-1} (scaled RCIS/6-31 result for the inversion mode for DCDMA). However, this result must be confirmed using results for DCDMA with a deuterated amino group. These experiments are in progress.

CONCLUSIONS

Available photophysical data for DCDMA in solution and ab initio quantum mechanical calculations (CIS/6-31G* and CASPT2 [31–33]) for vacuum-isolated molecules suggest that the transition to the singlet excited state of the DCDMA molecule in the spectral range 29,800–32,200 cm^{-1} represents a p-type transition. The fluorescence excitation spectrum of the jet-cooled DCDMA molecules has a very rich vibronic structure. Dominant features in the spectrum are connected with totally symmetric vibrational modes (5 at 112 cm^{-1}, 14 at 426 cm^{-1}, and 49 at 1569 cm^{-1}). The agreement between observed vibrational excited-state frequencies of the DCDMA molecule and the results of the ab initio CIS/6-31G* calculations is good. This result supports the conclusions that the ab initio CIS method is particularly suitable for calculations of the geometry and frequencies of the singlet excited states with a dominant HOMO-LUMO excited configuration [12,15,34,36].

Mode 5 involves symmetrical in-plane motions of CN groups adjacent to the amino group. The amino group undergoes geometry change upon electronic excitation (nonplanar in the ground state, planar in the excited state). The ab initio calculations of the vibrational modes in the ground state of the DCDMA molecule show that mode 5 involves symmetrical in-plane motions of the cyano groups and out-of-plane motions of the hydrogen atoms of the amino group. An important feature of this mode is that when the cyano groups move toward the amino group, the hydrogen atoms move toward the plane of the benzene ring. On the basis of the steric consideration, one should expect the motions of the hydrogen atoms to be in opposite directions. The significant intensities of these bands show that electronic excitation induces large changes in the interaction between adjacent amino and cyano substituents in the benzene ring. The hydrogen atoms of the amino group are engaged in hydrogen bonding with the cyano substituent. For DCDMA we find large shifts of the 00 transition upon deuterium exchange in the amino group. This also seems to support the notion of intramolecular hydrogen bonding. The evidence for intramolecular hydrogen bonding in the DCDMA molecule in the ground state can be found from the IR and Raman spectra.

ACKNOWLEDGMENTS

This work was supported by grants from the Polish State Committee for Scientific Research, 3T09A 124 09 and KBN/UJ/009/96. The authors thank Dr. Piotr Milart and Dr. Jan Boksa for the synthesis of 2,6-dicyano-3,5-dimethylaniline. P. Kolek would like to thank Dr. K. Boerve for an introduction to the field of quantum chemistry computations. We would also like to thank Dr. D. Birch for editorial comments.

REFERENCES

1. D. H. Levy (1980) *Annu. Rev. Phys. Chem.* **31**, 197.
2. R. E. Smally, L. Wharton, and D. H. Levy (1977) *Acc. Chem. Res.* **10**, 139.
3. J. M. Hayes (1987) *Chem. Rev.* **87**, 745.
4. V. Vaida (1986) *Acc. Chem. Res.* **19**, 114.
5. M. Ito, T. Ebata, and N. Mikami (1988) *Annu. Rev. Phys. Chem.* **39**, 123.
6. A. H. Zewail (1994) *Femtochemistry, Ultrafast Dynamics of the Chemical Bond, Vols. I, II*, Word Scientific, Singapore.

7. G. Herzberg (1966) *Molecular Spectra and Molecular Structure. III. Electronic Spectra and Electronic Structure of Polyatomic Molecules*, D. Van Nostrand, New York.
8. N. Mikami, A. Hiraya, I. Fujiwara, and M. Ito (1980) *Chem. Phys. Lett.* **74**, 531.
9. S. Zilberg, U. Asmuni, R. Fraenkel, and Y. Haas (1994) *Chem. Phys.* **186**, 303–316.
10. S. Zilberg and Y. Haas (1995) *J. Chem. Phys.* **103**, 20–36.
11. S. Mukamel (1988) *Adv. Chem. Phys.* **LXX**, 165–230.
12. Y. Haas, S. Kendler, E. Zingher, H. Zuckermann, and S. Zilberg (1995) *J. Chem. Phys.* **103**, 37–47.
13. A. Sobolewski, C. Woywod, and W. Domcke (1993) *J. Chem. Phys.* **98**, 5627–5641.
14. W. Siebrand, M. Z. Zgierski, F. Zerbetto, M. J. Wojcik, M. Boczar, T. Chkraborty, W. G. Kofron, and E. C. Lim (1997) *J. Chem. Phys.* **106**, 6279–6287.
15. G. S. Jas and K. Kuczera (1997) *Chem. Phys.* **214**, 229–241.
16. G. Stock, C. Woywod, W. Domcke, T. Swinney, and B. Hudson (1995) *J. Chem. Phys.* **103**, 6851–6860.
17. S. Wategaonkar and S. Doraiswamy (1996) *J. Chem. Phys.* **105**, 1786–1797.
18. J. I. Selco and P. G. Carrick (1995) *J. Mol. Spectrosc.* **173**, 262–276.
19. C. Dedonder-Lardeux, C. Jouvet, S. Martrenchard, D. Solgadi, J. McCombie, B. D. Howells, T. F. Palmer, A. Subaric-Leitis, C. Monte, W. Rettig, and P. Zimmermann (1995) *Chem. Phys.* **191**, 271–287.
20. A. L. Sobolewski (1990) *J. Chem. Phys.* **93**, 6433.
21. E. R. Th. Kerstel, M. Becucci, G. Pietraperza, and E. Castellucci (1995) *Chem. Phys.* **199**, 263–273.
22. J. B. Hopkins, D. E. Powers, and R. E. Smalley (1980) *J. Chem. Phys.* **72**, 5039–5048.
23. J. B. Hopkins, D. E. Powers, S. Mukamel, and R. E. Smalley (1980) *J. Chem. Phys.* **72**, 5049–5061.
24. D. A. Chernoff and S. A. Rice (1979) *J. Chem. Phys.* **70**, 2511–2520.
25. A. Hiraya and K. Shobatake (1991) *J. Chem. Phys.* **94**, 7700–7706.
26. B. Kim, C. P. Schick, and P. M. Weber (1995) *J. Chem. Phys.* **103**, 6903–6913.
27. J. Herbich, F. P. Salgado, R. P. H. Rettschnick, Z. R. Grabowski, and H. Wójtowicz (1991) *J. Phys. Chem.* **95**, 3491–3497.
28. D. Phillips (1997) *J. Photochem. Photobiol. A Chem.* **105**, 307–315.
29. A. L. Sobolewski and W. Domcke (1996) *Chem. Phys. Lett.* **250**, 428–436.
30. R. Hull, *J. Chem. Soc.* **1951**, 1136.
31. B. O. Roos (1987) in K. P. Lawley (Ed.), *Ab Initio Methods in Quantum Chemistry II*, John Willey & Sons, New York.
32. V. Kelö and M. Urban (1980) *Int. J. Quant. Chem.* **18**, 1431.
33. K. Anderson, P.-Å. Malmalmquist, B. O. Roos, A. J. Sadlej, and K. Woliński (1990) *J. Phys. Chem.* **94**, 5483.
34. F. Negri and M. Z. Zgierski (1996) *J. Chem. Phys.* **104**, 3486–3500.
35. P. Swiderek, G. Hohlneicher, S. A. Maluendes, and M. Dupuis (1993) *J. Chem. Phys.* **98**, 974–987.
36. S. Zilberg and Y. Haas (1995) *J. Chem. Phys.* **103**, 20–36.
37. F. Zerbetto and M. Z. Zgierski (1994) *J. Chem. Phys.* **101**, 1842–1851.
38. E. B. Wilson, J. C. Decius, and P. C. Cross (1959) *Molecular Vibrations*, McGraw–Hill, New York.
39. S. Shaik, S. Zilberg, and Y. Haas (1996) *Acc. Chem. Res.* **29**, 211–218.
40. G. Berden, W. L. Meerts, D. F. Plusquellic, I. Fujita, and D. W. Pratt (1996) *J. Chem. Phys.* **104**, 3935.
41. G. Varsanyi (1973) *Assignments of Vibrational Spectra of 700 Benzene Derivatives*, Akademiai Kiado, Budapest.